

Characteristics of dynamic waves in incompressible fluid regarding nonlinear Boiti-Leon-Manna-Pempinelli model

Md. Tarikul Islam

Hajee Mohammad Danesh Science and Technology University

Tara Rani Sarkar

Hajee Mohammad Danesh Science and Technology University

Farah Aini Abdullah

Universiti Sains Malaysia

J. F. Gómez-Aguilar (✉ jose.ga@cenidet.tecnm.mx)

CONACyT-Tecnológico Nacional de México/CENIDET

Research Article

Keywords: Wave solutions, solitons, improved tanh scheme, improved auxiliary equation approach, the new (3+1)-dimensional generalized nonlinear Boiti-Leon-Manna-Pempinelli model

Posted Date: January 24th, 2023

DOI: <https://doi.org/10.21203/rs.3.rs-2493706/v1>

License:   This work is licensed under a Creative Commons Attribution 4.0 International License.

[Read Full License](#)

Additional Declarations: No competing interests reported.

Characteristics of dynamic waves in incompressible fluid regarding nonlinear Boiti-Leon-Manna-Pempinelli model

Md. Tarikul Islam^{a,b}, Tara Rani Sarkar^a, Farah Aini Abdullah^b, J.F. Gómez-Aguilar^{c*}

^aDepartment of Mathematics, Hajee Mohammad Danesh Science and Technology University, Dinajpur, Bangladesh.

^bSchool of Mathematical Sciences, Universiti Sains Malaysia, Penang 11800, Malaysia.

^cCONACyT-Tecnológico Nacional de México/CENIDET, Interior Internado Palmira S/N, Col. Palmira, C.P. 62490, Cuernavaca, Morelos, México.

*jose.ga@cenidet.tecnm.mx

Abstract: Distinct models involving nonlinearity are mostly appreciated for illustrating intricate phenomena arise in the nature. The new (3+1)-dimensional generalized nonlinear Boiti-Leon-Manna-Pempinelli (BLMP) model describes the dynamical behaviors of nonlinear waves arise in incompressible fluid. This present effort deals with the well-known governing BLMP equation by adopting two efficient schemes, namely improved tanh and improved auxiliary equation. As a result, a variety of appropriate wave solutions are made available in different type functions. The gathered solutions are figured out to characterize their internal properties for depicting the relevant phenomena. Diverse wave profiles are noticed in 3D, 2D and contour sense after assigning parameter's values involved in the achieved solutions. The finding results are comparably different and general due to the existing wave solutions. The employed approaches perform in a great way to construct analytic wave solutions of considered evolution equation and deserve further use in relevant research area.

Keywords: Wave solutions, solitons, improved tanh scheme, improved auxiliary equation approach; the new (3+1)-dimensional generalized nonlinear Boiti-Leon-Manna-Pempinelli model.

Mathematics Subject Classifications: 35C08, 35R11

1. Introduction

The physical phenomena in various branches of science such as physical science, biological science, chemical science, and geo-science etc. can be modeled through the nonlinear evolution equations [1-4]. The nonlinear models are unraveled for wave solutions by imposing analytical as well as numerical schemes. In this context, several computational approaches have been developed by researchers. Instantly, Backlund transformation [5], first integral method [6], Jacobi elliptic function scheme [7, 8], extended simplest equation technique [9-11], F-expansion method [12, 13], trial equation scheme [14, 15], various rational (G'/G) -expansion tools [16-18], exp-function approach [19, 20], improved tanh approach [21], Darboux transformation approach [22], different Hirota schemes [23-27], Kudryashov technique [28] etc.

This present study is conducted by implementing two competent techniques such as improved tanh and improved auxiliary equation. The advised schemes are imposed on the new (3+1) BLMP equation stated as follows [29]:

$$(u_x + u_y + u_z)_t + a(u_x + u_y + u_z)_{xxx} + b(u_x(u_x + u_y + u_z))_x = 0, \quad (1.1)$$

where a and b are non-zero parameters; u stands for the wave function alongside time variable t and spatial variables x , y and z . Earlier, the (3+1)-dimensional nonlinear Boiti-Leon-Manna-Pempinelli model describing dynamical behavior of waves in incompressible fluid has been investigated by many researchers for appropriate solutions due to wide scientific importance. Instantly, Xu produced lump kink solutions, localized excitation solutions, and presented Painleve analysis [30]; breather and rational wave solutions have been constructed by Peng et al. [31]; the governing model has been studied by Osman and Wazwaz providing lump, breather, and mixed wave solutions [32]; Liu et al. have obtained several wave solutions [33];

Tang and Zai have studied the same model and found some periodic wave solutions [34], Darvishi et al. derived stair and step soliton solutions of the model [35].

The new (3+1) BLMP model (1.1) has been studied by Samir et al. providing few analytical solutions with the assistance of improved simple equation method [36]. We have employed improved tanh tool and improved auxiliary equation approach to unravel the mentioned-governing BLMP model. Consequently, various types of solitary wave solutions are found in a great way which might attracted scholars for further research.

2. Illustration of schemes

This section deals with a short note on the suggested techniques which are well-established and available in the literature.

2.1. Improved tanh approach

The improved tanh scheme is efficient and stated generally in the form

$$u(\xi) = \frac{\sum_{i=0}^n t_i \Omega^i(\xi) + \sum_{i=1}^n \tau_i \Omega^{-i}(\xi)}{\sum_{i=0}^n \epsilon_i \Omega^i(\xi) + \sum_{i=1}^n \varepsilon_i \Omega^{-i}(\xi)}, \quad (2.1.1)$$

where $\Omega(\xi)$ satisfies the auxiliary equation

$$\Omega'(\xi) = \Omega(\xi) + \delta. \quad (2.1.2)$$

Eq. (2.1.2) delivers the solutions as follows:

$$(i) \Omega(\xi) = -\sqrt{-\delta} \tanh(\sqrt{-\delta} \xi) \text{ or } \Omega(\xi) = -\sqrt{-\delta} \coth(\sqrt{-\delta} \xi), \delta < 0. \quad (2.1.3)$$

$$(ii) \Omega(\xi) = -1/\xi, \delta = 0. \quad (2.1.4)$$

$$(iii) \Omega(\xi) = \sqrt{\delta} \tan(\sqrt{\delta} \xi) \text{ or } \Omega(\xi) = -\sqrt{\delta} \cot(\sqrt{\delta} \xi), \delta > 0. \quad (2.1.5)$$

The working procedures of the competent tool (2.1.1) are available in Ref. [37].

2.2. Improved auxiliary equation technique

The improved auxiliary equation approach is reliable and stated as

$$u(\xi) = \frac{\sum_{i=0}^n c_i \lambda^{\psi(\xi)}}{\sum_{i=0}^n d_i \lambda^{\psi(\xi)}}, \quad (2.2.1)$$

where $\psi(\xi)$ satisfies the auxiliary equation

$$\psi'(\xi) = \frac{1}{\ln \lambda} \{p \lambda^{-\psi(\xi)} + q + r \lambda^{\psi(\xi)}\}. \quad (2.2.2)$$

Eq. (2.2.2) offers several distinct solutions [38]. The working procedures of the advised scheme (2.2.1) have been presented in detail in Ref. [39].

3. Extraction of wave solutions

The transformation for new wave variable is supposed to be $u(x, y, z, t) = u(\xi)$, where $\xi = x + y + z + wt$. Then Eq. (1.1) is reduced to

$$3wu'' + 3au^{(iv)} + 6bu'u'' = 0, \quad (3.1)$$

which is ODE considering only ξ as independent variable. Anti-derivative of Eq. (3.1) with integral constant zero leaves

$$3wu' + 3au''' + 3bu'^2 = 0. \quad (3.2)$$

Balancing principle between u''' and u'^2 yields $n = 1$. Thereupon, the advised schemes are employed as follows:

3.1. Improved tanh scheme

This tool suggests the solution expression

$$u(\xi) = \frac{\iota_0 + \iota_1 \Omega(\xi) + \tau_1 \Omega^{-1}(\xi)}{\epsilon_0 + \epsilon_1 \Omega(\xi) + \varepsilon_1 \Omega^{-1}(\xi)}. \quad (3.1.1)$$

Utilizing Eq. (3.1.1) alongside its derivatives in Eq. (3.2) harvests a polynomial in $\Omega(\xi)$. Then, connect each coefficient to zero and use Maple software to solve the found algebraic equations for involved parameters. Eq. (3.1.1) takes the parameters values and solutions of Eq. (2.1.2) to make sure the following groups of wave solutions:

Solution group 1: For the parameter's values $\iota_0 = 0$, $\tau_1 = \frac{\iota_1 \epsilon_0 (6a\epsilon_0 + b\iota_1)}{24a\epsilon_1^2}$, $\epsilon_1 = \frac{\epsilon_0 (6a\epsilon_0 + b\iota_1)}{24a\epsilon_1}$,

$w = -\frac{2\epsilon_0(6a\epsilon_0+b\iota_1)}{3\epsilon_1^2}$, $\delta = -\frac{\epsilon_0(6a\epsilon_0+b\iota_1)}{24a\epsilon_1^2}$, the accepted wave solutions are

$$u_1^1(\xi) = \frac{24a\epsilon_1^2\iota_1\delta\tanh(\sqrt{-\delta}\xi) - \iota_1\epsilon_0(6a\epsilon_0+b\iota_1)\coth(\sqrt{-\delta}\xi)}{24a\epsilon_1^2\epsilon_0\sqrt{-\delta} + 24a\epsilon_1^3\delta\tanh(\sqrt{-\delta}\xi) - \epsilon_0\epsilon_1(6a\epsilon_0+b\iota_1)\coth(\sqrt{-\delta}\xi)}, \delta < 0 \quad (3.1.2)$$

$$u_1^2(\xi) = \frac{24a\epsilon_1^2\iota_1\delta\coth(\sqrt{-\delta}\xi) - \iota_1\epsilon_0(6a\epsilon_0+b\iota_1)\tanh(\sqrt{-\delta}\xi)}{24a\epsilon_1^2\epsilon_0\sqrt{-\delta} + 24a\epsilon_1^3\delta\coth(\sqrt{-\delta}\xi) - \epsilon_0\epsilon_1(6a\epsilon_0+b\iota_1)\tanh(\sqrt{-\delta}\xi)}, \delta < 0 \quad (3.1.3)$$

$$u_1^3(\xi) = \frac{-24a\epsilon_1^2\iota_1 - \iota_1\epsilon_0(6a\epsilon_0+b\iota_1)\xi^2}{24a\epsilon_1^2\epsilon_0\xi - 24a\epsilon_1^3 - \epsilon_0\epsilon_1(6a\epsilon_0+b\iota_1)\xi^2}, \delta = 0 \quad (3.1.4)$$

$$u_1^4(\xi) = \frac{24a\epsilon_1^2\iota_1\delta\tan(\sqrt{\delta}\xi) + \iota_1\epsilon_0(6a\epsilon_0+b\iota_1)\cot(\sqrt{\delta}\xi)}{24a\epsilon_1^2\epsilon_0\sqrt{\delta} + 24a\epsilon_1^3\delta\tan(\sqrt{\delta}\xi) + \epsilon_0\epsilon_1(6a\epsilon_0+b\iota_1)\cot(\sqrt{\delta}\xi)}, \delta > 0 \quad (3.1.5)$$

$$u_1^5(\xi) = \frac{-24a\epsilon_1^2\iota_1\delta\cot(\sqrt{\delta}\xi) - \iota_1\epsilon_0(6a\epsilon_0+b\iota_1)\tan(\sqrt{\delta}\xi)}{24a\epsilon_1^2\epsilon_0\sqrt{\delta} - 24a\epsilon_1^3\delta\cot(\sqrt{\delta}\xi) - \epsilon_0\epsilon_1(6a\epsilon_0+b\iota_1)\tan(\sqrt{\delta}\xi)}, \delta > 0 \quad (3.1.6)$$

where $\xi = x + y + z - \frac{2\epsilon_0(6a\epsilon_0+b\iota_1)}{3\epsilon_1^2}t$.

Solution group 2: Due to the values $\iota_0 = 0$, $\tau_1 = 0$, $\epsilon_1 = 0$, $w = -\frac{2\epsilon_0(6a\epsilon_0+b\iota_1)}{3\epsilon_1^2}$, $\delta =$

$-\frac{\epsilon_0(6a\epsilon_0+b\iota_1)}{6a\epsilon_1^2}$, the gained solutions are presented as

$$u_2^1(\xi) = \frac{-\iota_1\sqrt{-\delta}\tanh(\sqrt{-\delta}\xi)}{\epsilon_0 - \epsilon_1\sqrt{-\delta}\tanh(\sqrt{-\delta}\xi)}, \delta < 0 \quad (3.1.7)$$

$$u_2^2(\xi) = \frac{-\iota_1\sqrt{-\delta}\coth(\sqrt{-\delta}\xi)}{\epsilon_0 - \epsilon_1\sqrt{-\delta}\coth(\sqrt{-\delta}\xi)}, \delta < 0 \quad (3.1.8)$$

$$u_2^3(\xi) = \frac{-\iota_1}{\epsilon_0\xi - \epsilon_1}, \delta = 0 \quad (3.1.9)$$

$$u_2^4(\xi) = \frac{\iota_1\sqrt{\delta}\tan(\sqrt{\delta}\xi)}{\epsilon_0 + \epsilon_1\sqrt{\delta}\tan(\sqrt{\delta}\xi)}, \delta > 0 \quad (3.1.10)$$

$$u_2^5(\xi) = \frac{-\iota_1\sqrt{\delta}\cot(\sqrt{\delta}\xi)}{\epsilon_0 - \epsilon_1\sqrt{\delta}\cot(\sqrt{\delta}\xi)}, \delta > 0 \quad (3.1.11)$$

where $\xi = x + y + z - \frac{2\epsilon_0(6a\epsilon_0+b\iota_1)}{3\epsilon_1^2}t$.

Solution group 3: The outcomes $\iota_0 = 0$, $\tau_1 = -\frac{36\epsilon_1^2\delta^2a^2}{\iota_1b^2}$, $\epsilon_0 = -\frac{6\epsilon_1^2\delta a}{\iota_1b}$, $\epsilon_1 = 0$, $w = 4a\delta$

offers the solutions

$$u_3^1(\xi) = \frac{\iota_1^2b^2 \tanh(\sqrt{-\delta}\xi) + 36\epsilon_1^2\delta a^2 \coth(\sqrt{-\delta}\xi)}{-6\epsilon_1^2ab\sqrt{-\delta} + \epsilon_1\iota_1b^2 \tanh(\sqrt{-\delta}\xi)}, \delta < 0 \quad (3.1.12)$$

$$u_3^2(\xi) = \frac{\iota_1^2b^2 \coth(\sqrt{-\delta}\xi) + 36\epsilon_1^2\delta a^2 \tanh(\sqrt{-\delta}\xi)}{-6\epsilon_1^2ab\sqrt{-\delta} + \epsilon_1\iota_1b^2 \coth(\sqrt{-\delta}\xi)}, \delta < 0 \quad (3.1.13)$$

$$u_3^3(\xi) = \frac{\iota_1^2b^2 \tan(\sqrt{\delta}\xi) - 36\epsilon_1^2\delta a^2 \cot(\sqrt{\delta}\xi)}{-6\epsilon_1^2ab\sqrt{\delta} + \epsilon_1\iota_1b^2 \tan(\sqrt{\delta}\xi)}, \delta > 0 \quad (3.1.14)$$

$$u_3^4(\xi) = \frac{-\iota_1^2b^2 \cot(\sqrt{\delta}\xi) + 36\epsilon_1^2\delta a^2 \tan(\sqrt{\delta}\xi)}{-6\epsilon_1^2ab\sqrt{\delta} - \epsilon_1\iota_1b^2 \cot(\sqrt{\delta}\xi)}, \delta > 0 \quad (3.1.15)$$

where $\xi = x + y + z + 4a\delta t$.

Solution group 4: Interleaving the results $\iota_0 = 0$, $\iota_1 = -\frac{\tau_1}{\delta}$, $\epsilon_0 = \frac{b\tau_1}{6a\delta}$, $\epsilon_1 = 0$, $\epsilon_1 = 0$, $w =$

$16a\delta$, the wave solutions are achieved as

$$u_4^1(\xi) = \frac{6a\sqrt{-\delta}\{\tanh(\sqrt{-\delta}\xi) + \coth(\sqrt{-\delta}\xi)\}}{b}, \delta < 0 \quad (3.1.16)$$

$$u_4^2(\xi) = \frac{6a\sqrt{-\delta}\{\coth(\sqrt{-\delta}\xi) + \tanh(\sqrt{-\delta}\xi)\}}{b}, \delta < 0 \quad (3.1.17)$$

$$u_4^3(\xi) = \frac{6a\sqrt{\delta}\{-\tan(\sqrt{\delta}\xi) + \cot(\sqrt{\delta}\xi)\}}{b}, \delta > 0 \quad (3.1.18)$$

$$u_4^4(\xi) = \frac{6a\sqrt{\delta}\{\cot(\sqrt{\delta}\xi) - \tan(\sqrt{\delta}\xi)\}}{b}, \delta > 0 \quad (3.1.19)$$

where $\xi = x + y + z + 16a\delta t$.

Solution group 5: Considering the agreements $\iota_0 = 0$, $\iota_1 = -\frac{6a\epsilon_0}{b}$, $\tau_1 = \frac{6a\epsilon_1^2}{b\epsilon_0}$, $\epsilon_1 = 0$, $w =$

$4a\delta$, we construct the solutions

$$u_5^1(\xi) = \frac{6a\{-\epsilon_0^2\delta \tanh(\sqrt{-\delta}\xi) - \epsilon_1^2 \coth(\sqrt{-\delta}\xi)\}}{b\epsilon_0\{\epsilon_0\sqrt{-\delta} - \epsilon_1 \coth(\sqrt{-\delta}\xi)\}}, \delta < 0 \quad (3.1.20)$$

$$u_5^2(\xi) = \frac{6a\{-\epsilon_0^2\delta \coth(\sqrt{-\delta}\xi) - \epsilon_1^2 \tanh(\sqrt{-\delta}\xi)\}}{b\epsilon_0\{\epsilon_0\sqrt{-\delta} - \epsilon_1 \tanh(\sqrt{-\delta}\xi)\}}, \delta < 0 \quad (3.1.21)$$

$$u_5^3(\xi) = \frac{6a\{-\epsilon_0^2\delta \tan(\sqrt{\delta}\xi) + \epsilon_1^2 \cot(\sqrt{\delta}\xi)\}}{b\epsilon_0\{\epsilon_0\sqrt{\delta} + \epsilon_1 \cot(\sqrt{\delta}\xi)\}}, \delta > 0 \quad (3.1.22)$$

$$u_5^4(\xi) = \frac{6a\{\epsilon_0^2\delta \cot(\sqrt{\delta}\xi) - \epsilon_1^2 \tan(\sqrt{\delta}\xi)\}}{b\epsilon_0\{\epsilon_0\sqrt{\delta} - \epsilon_1 \tan(\sqrt{\delta}\xi)\}}, \delta > 0 \quad (3.1.23)$$

where $\xi = x + y + z + 4a\delta t$.

Solution group 6: For the outcomes $\iota_0 = 0$, $\iota_1 = 0$, $\epsilon_0 = \frac{b\tau_1}{6a\delta}$, $\epsilon_1 = 0$, $\epsilon_1 = 0$, $w = 4a\delta$, the

wave solutions are found as

$$u_6^1(\xi) = \frac{6a\sqrt{-\delta} \coth(\sqrt{-\delta}\xi)}{b}, \delta < 0 \quad (3.1.24)$$

$$u_6^2(\xi) = \frac{6a\sqrt{-\delta} \tanh(\sqrt{-\delta}\xi)}{b}, \delta < 0 \quad (3.1.25)$$

$$u_6^3(\xi) = \frac{6a\sqrt{\delta} \cot(\sqrt{\delta}\xi)}{b}, \delta > 0 \quad (3.1.26)$$

$$u_6^4(\xi) = \frac{-6a\sqrt{\delta} \tan(\sqrt{\delta}\xi)}{b}, \delta > 0 \quad (3.1.27)$$

where $\xi = x + y + z + 4a\delta t$.

Solution group 7: According to the values $\iota_0 = 0$, $\iota_1 = 0$, $\tau_1 = \frac{6a(\delta\epsilon_0^2 + \epsilon_1^2)}{b\epsilon_0}$, $\epsilon_1 = 0$, $w = 4a\delta$,

we receive the results

$$u_7^1(\xi) = \frac{-6a(\delta\epsilon_0^2 + \epsilon_1^2) \coth(\sqrt{-\delta}\xi)}{b\epsilon_0\{\epsilon_0\sqrt{-\delta} - \epsilon_1 \coth(\sqrt{-\delta}\xi)\}}, \delta < 0 \quad (3.1.28)$$

$$u_7^2(\xi) = \frac{-6a(\delta\epsilon_0^2 + \epsilon_1^2) \tanh(\sqrt{-\delta}\xi)}{b\epsilon_0\{\epsilon_0\sqrt{-\delta} - \epsilon_1 \tanh(\sqrt{-\delta}\xi)\}}, \delta < 0 \quad (3.1.29)$$

$$u_7^3(\xi) = \frac{6a(\delta\epsilon_0^2 + \epsilon_1^2) \cot(\sqrt{\delta}\xi)}{b\epsilon_0\{\epsilon_0\sqrt{\delta} + \epsilon_1 \cot(\sqrt{\delta}\xi)\}}, \delta > 0 \quad (3.1.30)$$

$$u_7^4(\xi) = \frac{-6a(\delta\epsilon_0^2 + \epsilon_1^2) \tan(\sqrt{\delta}\xi)}{b\epsilon_0\{\epsilon_0\sqrt{\delta} - \epsilon_1 \tan(\sqrt{\delta}\xi)\}}, \delta > 0 \quad (3.1.31)$$

where $\xi = x + y + z + 4a\delta t$.

3.2. Improved auxiliary equation technique

The scheme advised the solution form

$$u(\xi) = \frac{c_0 + c_1 \lambda^{\Psi(\xi)}}{d_0 + d_1 \lambda^{\Psi(\xi)}}. \quad (3.2.1)$$

The utilization of Eq. (3.2.1) and its derivatives forces Eq. (3.2) to be a polynomial in $\lambda^{\Psi(\xi)}$.

This polynomial leaves algebraic equations after assigning its coefficients to zero. We use Maple software to obtain the considered parameters values. Combining these values and the solutions of Eq. (2.2.2) with Eq. (3.2.1) yields the following groups of wave solutions:

Solution group 1: The parameter's values $c_1 = -\frac{6apd_1^2 - 6aqd_0d_1 + 6ard_0^2 - bc_0d_1}{bd_0}$, $w = a(4pr - q^2)$ yields the solution expression

$$u_1(\xi) = \frac{bc_0d_0 - (6apd_1^2 - 6aqd_0d_1 + 6ard_0^2 - bc_0d_1)\lambda^{\Psi(\xi)}}{bd_0^2 + bd_0d_1\lambda^{\Psi(\xi)}}, \quad (3.2.2)$$

where $\xi = x + y + z + a(4pr - q^2)t$.

Under the assumption $q^2 - 4pr < 0$ and $r \neq 0$, we obtain

$$u_1^1(\xi) = \frac{2brc_0d_0 - (6apd_1^2 - 6aqd_0d_1 + 6ard_0^2 - bc_0d_1)\{-q + \sqrt{4pr - q^2}\tan(\sqrt{4pr - q^2}\xi/2)\}}{2brd_0^2 + bd_0d_1\{-q + \sqrt{4pr - q^2}\tan(\sqrt{4pr - q^2}\xi/2)\}}, \quad (3.2.3)$$

$$u_1^2(\xi) = \frac{2brc_0d_0 - (6apd_1^2 - 6aqd_0d_1 + 6ard_0^2 - bc_0d_1)\{-q - \sqrt{4pr - q^2}\cot(\sqrt{4pr - q^2}\xi/2)\}}{2brd_0^2 + bd_0d_1\{-q - \sqrt{4pr - q^2}\cot(\sqrt{4pr - q^2}\xi/2)\}}, \quad (3.2.4)$$

where $\xi = x + y + z + a(4pr - q^2)t$.

The postulates $q^2 - 4pr > 0$ and $r \neq 0$ provide

$$u_1^3(\xi) = \frac{2brc_0d_0 - (6apd_1^2 - 6aqd_0d_1 + 6ard_0^2 - bc_0d_1)\{-q - \sqrt{q^2 - 4pr}\tanh(\sqrt{q^2 - 4pr}\xi/2)\}}{2brd_0^2 + bd_0d_1\{-q - \sqrt{q^2 - 4pr}\tanh(\sqrt{q^2 - 4pr}\xi/2)\}}, \quad (3.2.5)$$

$$u_1^4(\xi) = \frac{2brc_0d_0 - (6apd_1^2 - 6aqd_0d_1 + 6ard_0^2 - bc_0d_1)\{-q - \sqrt{q^2 - 4pr}\coth(\sqrt{q^2 - 4pr}\xi/2)\}}{2brd_0^2 + bd_0d_1\{-q - \sqrt{q^2 - 4pr}\coth(\sqrt{q^2 - 4pr}\xi/2)\}}, \quad (3.2.6)$$

where $\xi = x + y + z + a(4pr - q^2)t$.

According to $q^2 + 4p^2 > 0$, $r \neq 0$ and $r = -p$, the wave solutions are

$$u_1^5(\xi) = \frac{2bpc_0d_0 - (6apd_1^2 - 6aqd_0d_1 - 6apd_0^2 - bc_0d_1)\{q + \sqrt{q^2 + 4p^2}\tanh(\sqrt{q^2 + 4p^2}\xi/2)\}}{2bpd_0^2 + bd_0d_1\{q + \sqrt{q^2 + 4p^2}\tanh(\sqrt{q^2 + 4p^2}\xi/2)\}}, \quad (3.2.7)$$

$$u_1^6(\xi) = \frac{2bpc_0d_0 - (6apd_1^2 - 6aqd_0d_1 - 6apd_0^2 - bc_0d_1)\{q + \sqrt{q^2 + 4p^2}\coth(\sqrt{q^2 + 4p^2}\xi/2)\}}{2bpd_0^2 + bd_0d_1\{q + \sqrt{q^2 + 4p^2}\coth(\sqrt{q^2 + 4p^2}\xi/2)\}}, \quad (3.2.8)$$

where $\xi = x + y + z - a(4p^2 + q^2)t$.

When $q^2 - 4p^2 < 0$ and $r = p$, we receive

$$u_1^7(\xi) = \frac{2bpc_0d_0 - (6apd_1^2 - 6aqd_0d_1 + 6apd_0^2 - bc_0d_1)\{-q + \sqrt{-q^2 + 4p^2}\tan(\sqrt{-q^2 + 4p^2}\xi/2)\}}{2bpd_0^2 + bd_0d_1\{-q + \sqrt{-q^2 + 4p^2}\tan(\sqrt{-q^2 + 4p^2}\xi/2)\}}, \quad (3.2.9)$$

$$u_1^8(\xi) = \frac{2bpc_0d_0 - (6apd_1^2 - 6aqd_0d_1 + 6apd_0^2 - bc_0d_1)\{-q + \sqrt{-q^2 + 4p^2}\cot(\sqrt{-q^2 + 4p^2}\xi/2)\}}{2bpd_0^2 + bd_0d_1\{-q + \sqrt{-q^2 + 4p^2}\cot(\sqrt{-q^2 + 4p^2}\xi/2)\}}, \quad (3.2.10)$$

where $\xi = x + y + z + a(4p^2 - q^2)t$.

The supposition $q^2 - 4p^2 > 0$ and $r = p$ serves

$$u_1^9(\xi) = \frac{2bpc_0d_0 - (6apd_1^2 - 6aqd_0d_1 + 6apd_0^2 - bc_0d_1)\{-q - \sqrt{q^2 - 4p^2}\tanh(\sqrt{q^2 - 4p^2}\xi/2)\}}{2bpd_0^2 + bd_0d_1\{-q - \sqrt{q^2 - 4p^2}\tanh(\sqrt{q^2 - 4p^2}\xi/2)\}}, \quad (3.2.11)$$

$$u_1^{10}(\xi) = \frac{2bpc_0d_0 - (6apd_1^2 - 6aqd_0d_1 + 6apd_0^2 - bc_0d_1)\{-q - \sqrt{q^2 - 4p^2}\coth(\sqrt{q^2 - 4p^2}\xi/2)\}}{2bpd_0^2 + bd_0d_1\{-q - \sqrt{q^2 - 4p^2}\coth(\sqrt{q^2 - 4p^2}\xi/2)\}}, \quad (3.2.12)$$

where $\xi = x + y + z + a(4p^2 - q^2)t$.

The consideration $rp < 0$, $q = 0$ and $r \neq 0$ gives the solutions

$$u_1^{11}(\xi) = \frac{bc_0d_0 + (6apd_1^2 + 6ard_0^2 - bc_0d_1)\{\sqrt{-p/r}\tanh(\sqrt{-rp}\xi)\}}{bd_0^2 - bd_0d_1\{\sqrt{-p/r}\tanh(\sqrt{-rp}\xi)\}}, \quad (3.2.13)$$

$$u_1^{12}(\xi) = \frac{bc_0d_0 + (6apd_1^2 + 6ard_0^2 - bc_0d_1)\{\sqrt{-p/r}\coth(\sqrt{-rp}\xi)\}}{bd_0^2 - bd_0d_1\{\sqrt{-p/r}\coth(\sqrt{-rp}\xi)\}}, \quad (3.2.14)$$

where $\xi = x + y + z + 4aprt$.

Under the agreements $q = 0$ and $p = -r$, the attained solutions are

$$u_1^{13}(\xi) = \frac{bc_0d_0(1-e^{2r\xi}) - (-6ard_1^2 + 6ard_0^2 - bc_0d_1)(1+e^{2r\xi})}{bd_0^2(1-e^{2r\xi}) + bd_0d_1(1+e^{2r\xi})}, \quad (3.2.15)$$

where $\xi = x + y + z - 4ar^2t$.

For the condition $p = r = 0$, the wave solution is

$$u_1^{14}(\xi) = \frac{bc_0d_0 + (6aqd_0d_1 + bc_0d_1)\{\cosh(q\xi) + \sinh(q\xi)\}}{bd_0^2 + bd_0d_1\{\cosh(q\xi) + \sinh(q\xi)\}}, \quad (3.2.16)$$

where $\xi = x + y + z - aq^2t$.

If we agree $p = q = k$ and $r = 0$, then

$$u_1^{15}(\xi) = \frac{bc_0d_0 - (6akd_1^2 - 6akd_0d_1 - bc_0d_1)(e^{k\xi} - 1)}{bd_0^2 + bd_0d_1(e^{k\xi} - 1)}, \quad (3.2.17)$$

where $\xi = x + y + z - ak^2t$.

When $q = r = k$ and $p = 0$,

$$u_1^{16}(\xi) = \frac{bc_0d_0(1-e^{k\xi}) - (-6akd_0d_1 + 6akd_0^2 - bc_0d_1)(e^{k\xi})}{bd_0^2(1-e^{k\xi}) + bd_0d_1(e^{k\xi})}, \quad (3.2.18)$$

where $\xi = x + y + z - ak^2t$.

If $q = p + r$ is assumed, then we find

$$u_1^{17}(\xi) = \frac{bc_0d_0\{1-re^{(p-r)\xi}\} + (6apd_1^2 - 6apd_0d_1 - 6ard_0d_1 + 6ard_0^2 - bc_0d_1)\{1-pe^{(p-r)\xi}\}}{bd_0^2\{1-re^{(p-r)\xi}\} - bd_0d_1\{1-pe^{(p-r)\xi}\}}, \quad (3.2.19)$$

where $\xi = x + y + z - a(p-r)^2t$.

After letting the supposition $q = -(p+r)$, the wave solution is

$$u_1^{18}(\xi) = \frac{bc_0d_0\{r-e^{(p-r)\xi}\} - (6apd_1^2 + 6apd_0d_1 + 6ard_0d_1 + 6ard_0^2 - bc_0d_1)\{p-e^{(p-r)\xi}\}}{bd_0^2\{r-e^{(p-r)\xi}\} + bd_0d_1\{p-e^{(p-r)\xi}\}}, \quad (3.2.20)$$

where $\xi = x + y + z - a(p-r)^2t$.

When $p = 0$, we receive the solution

$$u_1^{19}(\xi) = \frac{bc_0d_0(1-re^{q\xi})-(6ard_0d_1+6ard_0^2-bc_0d_1)(qe^{q\xi})}{bd_0^2(1-re^{q\xi})+bd_0d_1(qe^{q\xi})}, \quad (3.2.21)$$

where $\xi = x + y + z - aq^2t$.

The agreements $r = q = p \neq 0$ provide

$$u_1^{20}(\xi) = \frac{2bc_0d_0-(6apd_1^2-6aqd_0d_1+6ard_0^2-bc_0d_1)\{\sqrt{3}\tan(\sqrt{3}p\xi/2)-1\}}{2bd_0^2+bd_0d_1\{\sqrt{3}\tan(\sqrt{3}p\xi/2)-1\}}, \quad (3.2.22)$$

where $\xi = x + y + z + a(4pr - q^2)t$.

According to the condition $r = p$ and $q = 0$, the gained solution is

$$u_1^{21}(\xi) = \frac{bc_0d_0-(6apd_1^2+6apd_0^2-bc_0d_1)\tan(p\xi)}{bd_0^2+bd_0d_1\tan(p\xi)}, \quad (3.2.23)$$

where $\xi = x + y + z + 4ap^2t$.

Under the hypothesis $r = 0$, the exponential function solution is

$$u_1^{22}(\xi) = \frac{bc_0d_0-(6apd_1^2-6aqd_0d_1-bc_0d_1)(e^{q\xi}-m/n)}{bd_0^2+bd_0d_1(e^{q\xi}-m/n)}, \quad (3.2.24)$$

where $\xi = x + y + z - aq^2t$.

Solution group 2: The outcomes $c_0 = \frac{6apd_1}{b}$, $d_0 = 0$, $w = a(4pr - q^2)$ ensured the expression for desired wave solutions as

$$u_2(\xi) = \frac{c_1}{d_1} + \frac{6ap}{b\lambda\Psi(\xi)}, \quad (3.2.25)$$

where $\xi = x + y + z + a(4pr - q^2)t$.

The postulates $q^2 - 4pr < 0$ and $r \neq 0$ produce the wave solutions

$$u_2^1(\xi) = \frac{c_1}{d_1} + \frac{12apr}{b\{-q+\sqrt{4pr-q^2}\tan(\sqrt{4pr-q^2}\xi/2)\}}, \quad (3.2.26)$$

$$u_2^2(\xi) = \frac{c_1}{d_1} + \frac{12apr}{b\{-q-\sqrt{4pr-q^2}\cot(\sqrt{4pr-q^2}\xi/2)\}}, \quad (3.2.27)$$

where $\xi = x + y + z + a(4pr - q^2)t$.

According to the assumption $q^2 - 4pr > 0$ and $r \neq 0$, we receive

$$u_2^3(\xi) = \frac{c_1}{d_1} + \frac{12apr}{b\{-q - \sqrt{q^2 - 4pr} \tanh(\sqrt{q^2 - 4pr}\xi/2)\}}, \quad (3.2.28)$$

$$u_2^4(\xi) = \frac{c_1}{d_1} + \frac{12apr}{b\{-q - \sqrt{q^2 - 4pr} \coth(\sqrt{q^2 - 4pr}\xi/2)\}}, \quad (3.2.29)$$

where $\xi = x + y + z + a(4pr - q^2)t$.

For the conditions $q^2 + 4p^2 > 0$, $r \neq 0$ and $r = -p$, the attained solutions are

$$u_2^5(\xi) = \frac{c_1}{d_1} + \frac{12ap^2}{b\{q + \sqrt{q^2 + 4p^2} \tanh(\sqrt{q^2 + 4p^2}\xi/2)\}}, \quad (3.2.30)$$

$$u_2^6(\xi) = \frac{c_1}{d_1} + \frac{12ap^2}{b\{q + \sqrt{q^2 + 4p^2} \coth(\sqrt{q^2 + 4p^2}\xi/2)\}}, \quad (3.2.31)$$

where $\xi = x + y + z - a(4p^2 + q^2)t$.

The solutions according to $q^2 - 4p^2 < 0$ and $r = p$ are

$$u_2^7(\xi) = \frac{c_1}{d_1} + \frac{12ap^2}{b\{-q + \sqrt{-q^2 + 4p^2} \tan(\sqrt{-q^2 + 4p^2}\xi/2)\}}, \quad (3.2.32)$$

$$u_2^8(\xi) = \frac{c_1}{d_1} + \frac{12ap^2}{b\{-q + \sqrt{-q^2 + 4p^2} \cot(\sqrt{-q^2 + 4p^2}\xi/2)\}}, \quad (3.2.33)$$

where $\xi = x + y + z + a(4p^2 - q^2)t$.

When $q^2 - 4p^2 > 0$ and $r = p$,

$$u_2^9(\xi) = \frac{c_1}{d_1} + \frac{12ap^2}{b\{-q - \sqrt{q^2 - 4p^2} \tanh(\sqrt{q^2 - 4p^2}\xi/2)\}}, \quad (3.2.34)$$

$$u_2^{10}(\xi) = \frac{c_1}{d_1} + \frac{12ap^2}{b\{-q - \sqrt{q^2 - 4p^2} \coth(\sqrt{q^2 - 4p^2}\xi/2)\}}, \quad (3.2.35)$$

where $\xi = x + y + z + a(4p^2 - q^2)t$.

For the supposition $rp < 0$, $q = 0$ and $r \neq 0$, we obtain

$$u_2^{11}(\xi) = \frac{c_1}{d_1} - \frac{6ap}{b\{\sqrt{-p/r}\tanh(\sqrt{-rp}\xi)\}}, \quad (3.2.36)$$

$$u_2^{12}(\xi) = \frac{c_1}{d_1} - \frac{6ap}{b\{\sqrt{-p/r}\coth(\sqrt{-rp}\xi)\}}, \quad (3.2.37)$$

where $\xi = x + y + z + 4aprt$.

According to the assumptions $q = 0$ and $p = -r$, we attain

$$u_2^{13}(\xi) = \frac{c_1}{d_1} - \frac{6ar(1-e^{2r\xi})}{b(1+e^{2r\xi})}, \quad (3.2.38)$$

where $\xi = x + y + z - 4ar^2t$.

The postulates $p = q = k$ and $r = 0$ provide the solutions

$$u_2^{14}(\xi) = \frac{c_1}{d_1} + \frac{6ak}{b(e^{k\xi}-1)}, \quad (3.2.39)$$

where $\xi = x + y + z - ak^2t$.

The supposition $q = p + r$, yields

$$u_2^{15}(\xi) = \frac{c_1}{d_1} - \frac{6ap\{1-re^{(p-r)\xi}\}}{b\{1-pe^{(p-r)\xi}\}}, \quad (3.2.40)$$

where $\xi = x + y + z - a(p-r)^2t$.

The wave solution under the condition $q = -(p+r)$ is

$$u_2^{16}(\xi) = \frac{c_1}{d_1} + \frac{6ap\{r-e^{(p-r)\xi}\}}{b\{p-e^{(p-r)\xi}\}}, \quad (3.2.41)$$

where $\xi = x + y + z - a(p-r)^2t$.

Due to the assumption $r = q = p \neq 0$, we receive

$$u_2^{17}(\xi) = \frac{c_1}{d_1} + \frac{12ap}{b\{\sqrt{3}\tan\left(\frac{\sqrt{3}p\xi}{2}\right)-1\}}, \quad (3.2.42)$$

where $\xi = x + y + z + a(4pr - q^2)t$.

Considering the relations $r = p$ and $q = 0$, the solution is appeared as

$$u_2^{18}(\xi) = \frac{c_1}{d_1} + \frac{6ap}{b \tan(p\xi)}, \quad (3.2.43)$$

where $\xi = x + y + z + 4ap^2t$.

Under the supposition $r = 0$, the wave solution is

$$u_2^{19}(\xi) = \frac{c_1}{d_1} + \frac{6ap}{b(e^{q\xi} - m/n)}, \quad (3.2.44)$$

where $\xi = x + y + z - aq^2t$.

Remarks: The considered governing model (1.1) is demonstrated by utilizing two well-established approaches such as improved tanh and improved auxiliary equation. This present work provides a variety of wave solutions which are distinct and general than earlier finding results [36].

4. Graphical representations

The graphical representations of wave solutions are appreciated for depicting internal characteristics of nonlinear phenomena. In this consideration, we figure out the achieved wave solutions in 3D, 2D and contour profiles under the fixed values of the involved parameters. Fig 1(a), Fig 1(c) represent 3D and contour standing as anti-cuspon soliton for solution (3.1.4) under the values $\delta = y = z = 0, \epsilon_0 = -0.5, \epsilon_1 = a = b = 1, \iota_1 = -0.75$ in the range $-5 \leq x \leq 5, -0.5 \leq t \leq 8.5$ while 2D profile is found for $t = 0$ exposed in Fig 1(b). The soliton for solution (3.1.6) gives the periodic shape in which Fig 2(a), Fig 2(c) illustrate 3D and contour for the unknown values $\delta = \epsilon_0 = 0.5, \epsilon_1 = a = -1, \iota_1 = 0.1, b = -2, y = z = 0$ within the interval $-5 \leq x, t \leq 5$ while Fig 2(b) exhibit 2D plot together with $t = 0$. Fig 3(a), Fig 3(c) signifies 3D and contour provides the form of anti-bell shape soliton for solution (3.1.12) for the values $\delta = -0.25, \epsilon_1 = 0.5, \iota_1 = 1, a = -1, b = 2, y = z = 0$ in the range $-1 \leq x, t \leq 1$ while 2D graph is described for $t = 0$ in Fig 3(c). Fig 4(a), Fig 4(c) proceeds 3D and contour

stands for the shape of singular kink soliton for solution (3.1.21) under $\delta = -0.5, a = 0.25, b = -1, \epsilon_0 = 1, \epsilon_1 = 2, y = z = 0$ within $-3 \leq x, t \leq 3$ and 2D plot is displayed in Fig 4(b) for $t = 0$. The anti-kink shape soliton for solution (3.1.25) proceeds 3D and contour exposed in Fig 5(a), Fig 5(c) for the assumptions $\delta = a = -1, b = 1, y = z = 0$ in the interval $-3 \leq x, t \leq 3$ at the same time Fig 5(b) represents 2D graph along with $t = 0$. Fig 6(a), Fig 6(c) represent 3D and contour expressed as periodic soliton for solution (3.2.10) for the values chosen as $p = r = b = d_0 = 1, q = a = c = d_1 = -1, y = z = 0$ in the range $-3 \leq x, t \leq 3$ while 2D graph is shown for $t = 0$ exposed in Fig 6(b). (3.2.21) proceeds the form of singular kink soliton exposed in Fig 7(a), Fig 7(c) as 3D and contour for the assumptions $p = y = z = 0, r = b = c_0 = d_0 = d_1 = 1, q = a = -1$ in the interval $-3 \leq x, t \leq 3$ and 2D profile is revealed in Fig 7(b) for $t = 0$. Fig 8(a), Fig 8(c) exposed 3D and contour standing as periodic soliton for solution (3.2.33) for the unknown values $p = r = a = c_1 = -1, q = b = d_1 = 1, y = z = 0$ within $-3 \leq x, t \leq 3$ while 2D plot is shown for $t = 0$ obtained in the Fig 8(b). The soliton for solution (3.2.39) gives anti-bell shape exposed in Fig 9(a), Fig 9(c) proceeds 3D and contour under the values $k = p = q = d_1 = 1, r = y = z = 0, a = b = c_1 = -1$ in the interval $-13 \leq x, t \leq 13$ in which Fig 9(b) disclose 2D plot in association with $t = 0$. Fig 10(a), Fig 10(c) represent 3D and contour expressed as kink soliton for solution (3.2.41) for the unknown values $p = q = -0.5, r = a = c_1 = d_1 = 1, b = -1, y = z = 0$ within the range $-13 \leq x, t \leq 13$ where 2D plot is displayed for $t = 0$ revealed in Fig 10(b).

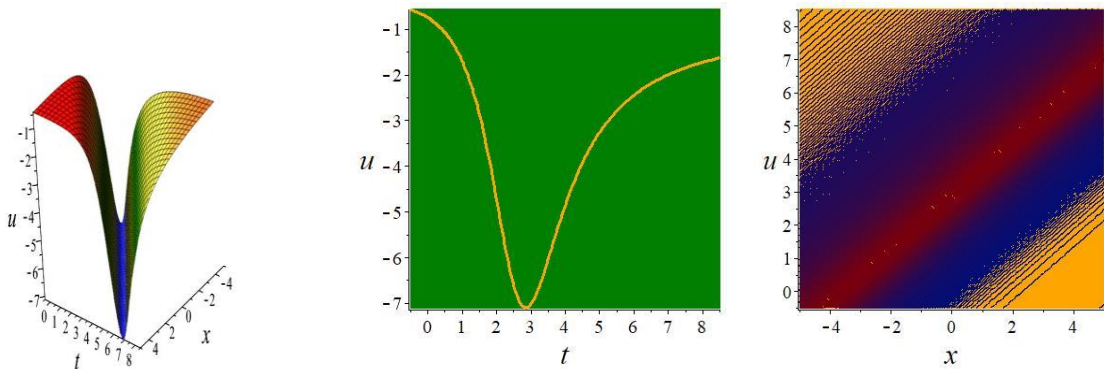


Fig 1(a)

Fig 1(b)

Fig 1(c)

The soliton for solution (3.1.4) is in anti-cuspon shape for $\delta = y = z = 0, \epsilon_0 = -0.5, \epsilon_1 = a = b = 1, t_1 = -0.75$ in the range $-5 \leq x \leq 5, -0.5 \leq t \leq 8.5$ while 2D plot is described in Fig 1(b) for $t = 0$.

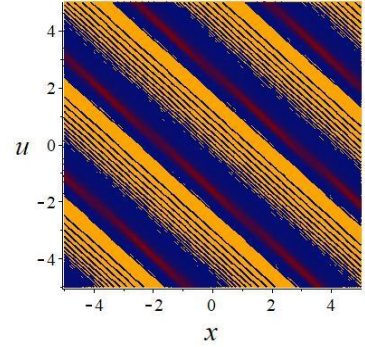
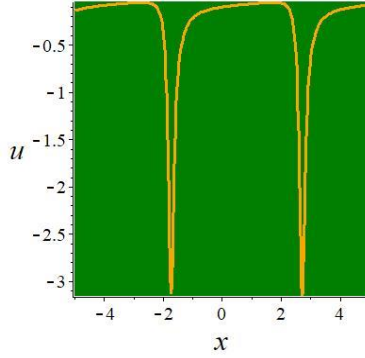
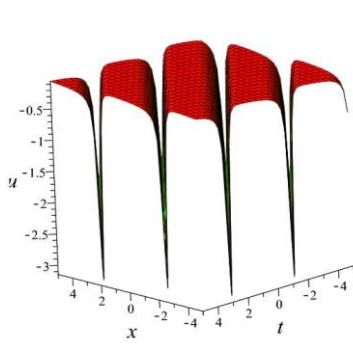


Fig 2(a)

Fig 2(b)

Fig 2(c)

Plot the solution (3.1.6) represents periodic shape for the unknown values $\delta = \epsilon_0 = 0.5, \epsilon_1 = a = -1, t_1 = 0.1, b = -2, y = z = 0$ within the interval $-5 \leq x, t \leq 5$ in which Fig 2(b) exhibit 2D plot together with $t = 0$.

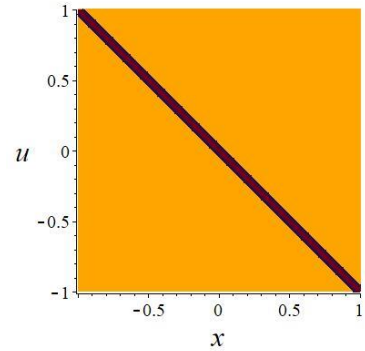
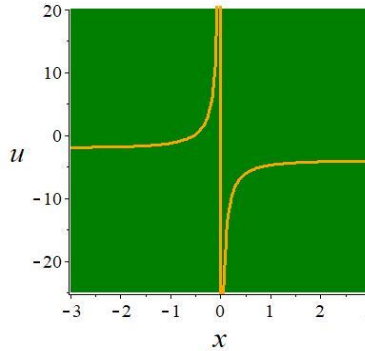
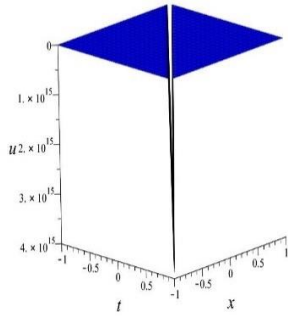


Fig 3(a)

Fig 3(b)

Fig 3(c)

The soliton for solution (3.1.12) is in anti-bell type under $\delta = -0.25, \epsilon_1 = 0.5, t_1 = 1, a = -1, b = 2, y = z = 0$ within the range $-1 \leq x, t \leq 1$ while Fig 3(b) represents 2D plot along with $t = 0$.

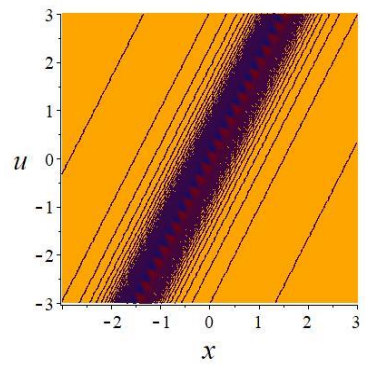
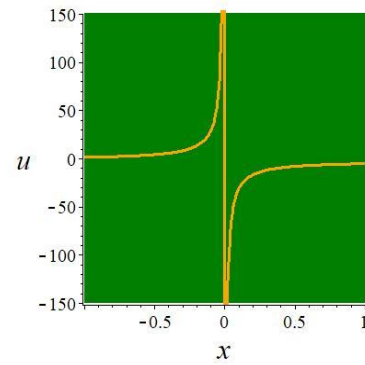
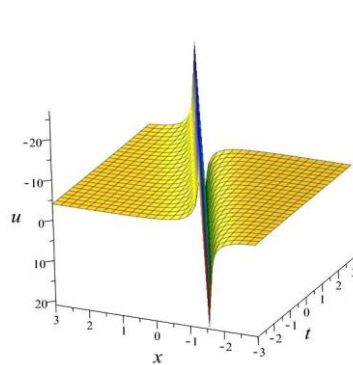


Fig 4(a)

Fig 4(b)

Fig 4(c)

The singular kink type soliton of solution (3.1.21) stands for $\delta = -0.5, a = 0.25, b = -1, \epsilon_0 = 1, \epsilon_1 = 2, y = z = 0$ within $-3 \leq x, t \leq 3$ and 2D plot is displayed in Fig 4(b) for $t = 0$.

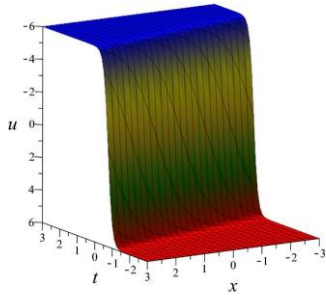


Fig 5(a)

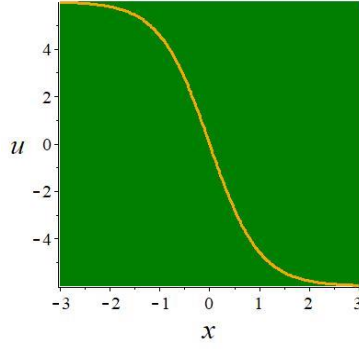


Fig 5(b)

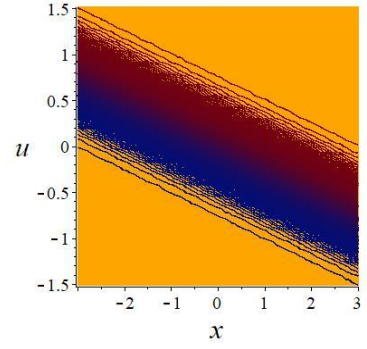


Fig 5(c)

The anti-kink type soliton of solution (3.1.25) for the unknown values $\delta = a = -1, b = 1, y = z = 0$ in the range $-3 \leq x, t \leq 3$ at the same time Fig 5(b) represents 2D graph along with $t = 0$.

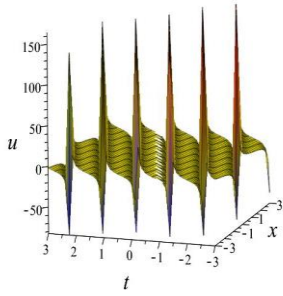


Fig 6(a)

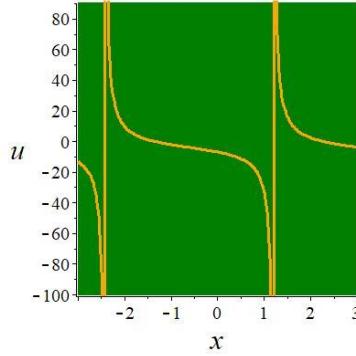


Fig 6(b)

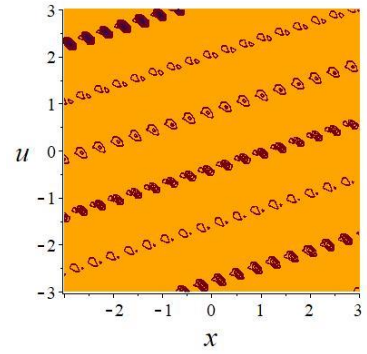


Fig 6(c)

Sketch of (3.2.10) stands for periodic shape for unknown values chosen are $p = r = b = d_0 = 1, q = a = c = d_1 = -1, y = z = 0$ in the range $-3 \leq x, t \leq 3$ and 2D graph is shown in the Fig 6(b) for $t = 0$.

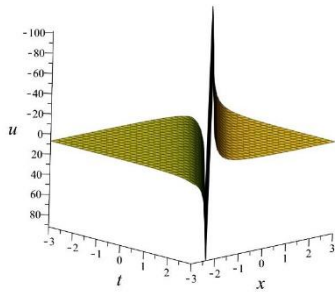


Fig 7(a)

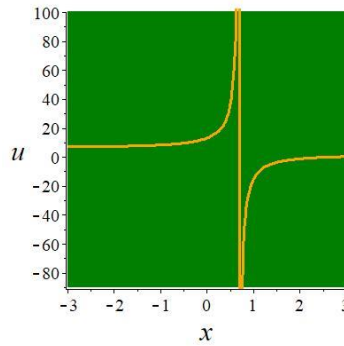


Fig 7(b)

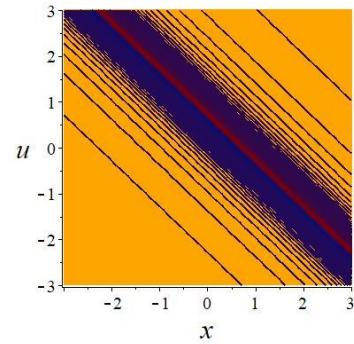


Fig 7(c)

The singular kink shape soliton of solution (3.2.21) for the assumptions $p = y = z = 0, r = b = c_0 = d_0 = d_1 = 1, q = a = -1$ in the interval $-3 \leq x, t \leq 3$ and Fig 7(b) represents 2D plot for $t = 0$.

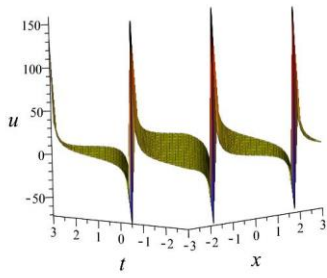


Fig 8(a)

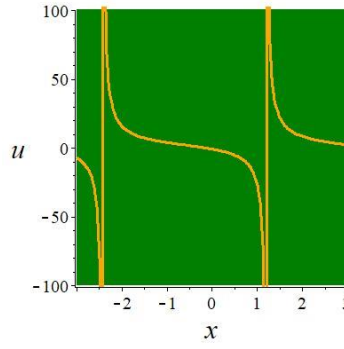


Fig 8(b)

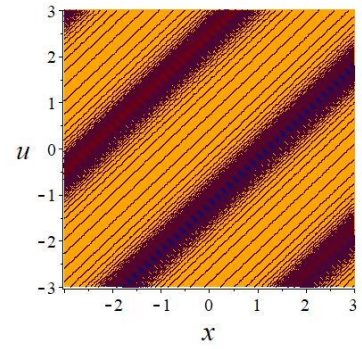


Fig 8(c)

Plot the solution (3.2.33) displays periodic graph for the values $p = r = a = c_1 = -1, q = b = d_1 = 1, y = z = 0$ within $-3 \leq x, t \leq 3$ and 2D plot is obtained in the Fig 8(b) for $t = 0$.

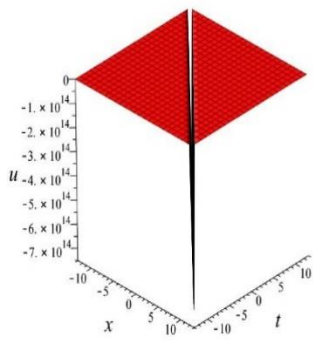


Fig 9(a)

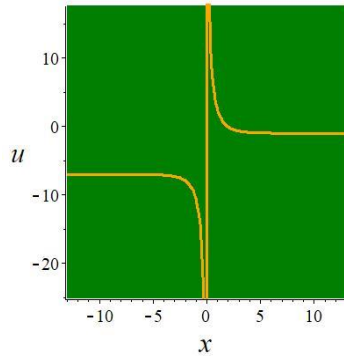


Fig 9(b)

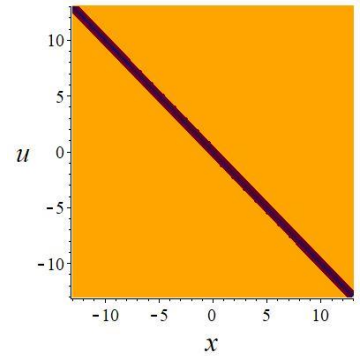


Fig 9(c)

Sketch of (3.2.39) stands for anti-bell shape for the assumptions $k = p = q = d_1 = 1, r = y = z = 0, a = b = c_1 = -1$ within $-13 \leq x, t \leq 13$ in which Fig 9(b) disclose 2D plot in association with $t = 0$.

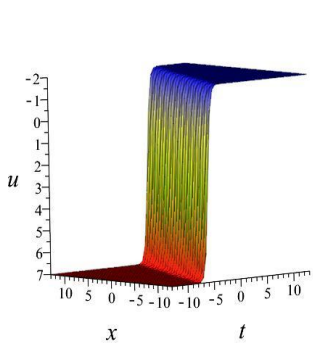


Fig 10(a)

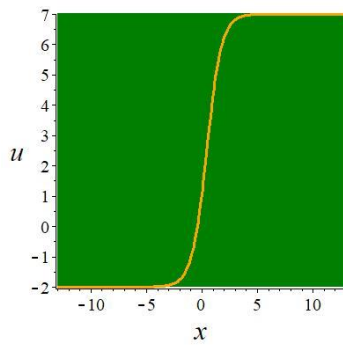


Fig 10(b)

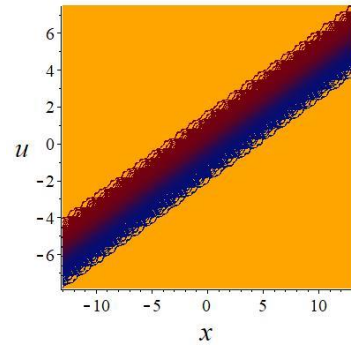


Fig 10(c)

Soliton of the solution (3.2.41) is in kink shape for the values $p = q = -0.5, r = a = c_1 = d_1 = 1, b = -1, y = z = 0$ within the interval $-13 \leq x, t \leq 13$ where Fig 10(b) is displayed for 2D plot along with $t = 0$.

5. Conclusions

The exploration achieves the goal providing the desired various solitary wave solutions of the BLMP model. The stated model has adopted improved tanh and improved auxiliary equation approaches for leaving appropriate traveling wave solutions. The acquired solutions have been compared with earlier results to express diversity and generality. The BLMP equation is significant for describing the behavior of nonlinear dynamic waves arise in incompressible fluid. Taking this into consideration, the obtained solutions have been plotted in 3D, 2D and contour profiles appearing as periodic, singular periodic, bell, anti-bell, cuspon, peakon, kink, anti-kink etc. The entire study might be considered as significant and interesting for presenting a great combination of well-known nonlinear BLMP equation and advised powerful techniques.

Acknowledgments

José Francisco Gómez Aguilar acknowledges the support provided by CONACyT: Cátedras CONACyT para jóvenes investigadores 2014 and SNI-CONACyT.

Declarations

Ethical Approval

Not applicable

Competing interests

The authors state that there are no competing interests.

Authors' contributions

Md. Tarikul Islam: Conceptualization, methodology, validation, investigation, Writing-original draft preparation, writing-review; Tara Rani Sarkar: Conceptualization, methodology, validation, Writing-original draft preparation, writing-review; Farah Aini Abdullah: Validation, formal analysis, investigation; J.F. Gómez-Aguilar: Conceptualization,

methodology, validation, writing-review and editing. All authors have read and agreed to the published version of the manuscript.

Funding

Not applicable

Declarations

Conflict of interest. The authors declare that there is no conflict of interests regarding the publication of this paper.

Availability of data and materials

Not applicable

References

1. A.A. Kilbas, H.M. Srivastava and J.J. Trujillo. Theory and applications of fractional differential equations. Elsevier, Amsterdam, (2006).
2. J.Y. Yang, W.X. Ma and C.M. Khalique. Determining lump solutions for a combined soliton equation in (2+1)-dimensions. *Eur. Phys. J. Plus.*, 135, 494-506 (2020).
3. A.M. Wazwaz Partial differential equations: Method and applications. Taylor and Francis, (2002).
4. M. Bilal, A.R. Seadawy, M. Younis, S.T.R. Rizvi, K. El-Rashidy, S.F. Mahmoud, Analytical wave structures in plasma physics modelled by Gilson-Pickering equation by two integration norms. *Res. Phys.*, 23, 103959 (2021).
5. A. Arnous, M. Mirzazadeh and M. Eslami. Exact solutions of the Drinfel'd-Sokolov-Wilson equation using Backlund transformation of Riccati equation and trial function approach. *Pramana*, 86 (6), 1153-1160 (2016).
6. Q. Zhang, M. Xiong and L. Chen. Exact solutions of two nonlinear partial differential equations by the first integral method. *Adv. Pure Math.*, 10, 12 (2020).

7. M. El-Sheikh, H.M. Ahmed, A.H. Arnous and W.B. Rabie. Optical solitons and other solutions in birefringent fibers with Biswas-Arshed equation by Jacobi's elliptic function approach. *Optik*, 202, 163546 (2020).
8. H.M. Ahmed, W.B. Rabie and M.A. Ragusa. Optical solitons and other solutions to kaup-Newell equation with Jacobi elliptic function expansion method. *Anal. Math. Phys.*, 11 (1), 1-16 (2021).
9. M. El-Sheikh, H.M. Ahmed, A.H. Arnous, W.B. Rabie, A. Biswas, S. Khan and A.S. Alshomrani. Optical solitons with differential group delay for coupled kundu- Eckhaus equation using extended simplest equation approach. *Optik*, 208, 164051 (2020).
10. H.M. Ahmed, W.B. Rabie, A.H. Arnous and A.M. Wazwaz. Optical solitons in birefringent fibers of kaup-Newell's equation with extended simplest equation method. *Phys. Scr.*, 95 (11), 115214 (2020).
11. D. Lu, A. Seadawy and M. Arshad. Applications of extended simple equation method on unstable nonlinear Schrodinger equations. *Optik*, 140, 136-144 (2017).
12. V. Apriliani, I. Maulidi and B. Azhari. Extended F-expansion method for solving the modified Korteweg-de-Vries (mkdV) equation. *Al-Jabar: J. Pendidik. Mat.*, 11 (1), 93-100 (2020).
13. Y. Yildirim. Optical solutions with Biswas-Arshed equation by F-expansion method. *Optik*, 227, 165788 (2021).
14. Y. Yildirim. Optical solitons to Chen-Lee-Liu model with trial equation approach. *Optik*, 183, 849-853 (2019).
15. A. Biswas, M. Ekici, A. Sonmezoglu, A.S. Alshomrani and M.R. Belic. Optical solitons with Kudryashov's equation by extended trial function. *Optik*, 202, 163290 (2020).

16. M.A. Akbar, F.A. Abdullah, M.T. Islam, M.A. Al-Sharif and M.S. Osman. New solutions of the soliton type of shallow water waves and superconductivity models. *Res. Phys.* 44 106180 (2023).
17. M.N. Alam and X. Li. New soliton solutions to the nonlinear complex fractional Schrodinger equation and the conformable time-fractional Klein-Gordon equation with quadratic and cubic nonlinearity. *Phys. Scr.*, 95 (4), 045224 (2020).
18. I. Samir, N. Badra, A.R. Seadawy, H.M. Ahmed and A.H. Arnous. Exact wave solutions of the fourth order non-linear partial differential equation of optical fiber pulses by using different methods. *Optik*, 230, 166313 (2021).
19. M. Hafez and M. Akbar. An exponential expansion method and its application to the strain wave equation in microstructured solids. *Ain Shams Eng. J.*, 6 (2), 683-690 (2015).
20. H.M. Ahmed, M. El-Sheikh, A.H. Arnous and W.B. Rabie. Solitons and other solutions to $(n+1)$ -dimensional modified Zakharov-Kuznetsov equation by exp-function method. *SeMA J.*, 78 (1), 1-13 (2020).
21. F.A. Abdullah, M.T. Islam, J.F.G. Aguilar and M.A. Akbar. Impressive and innovative soliton shapes for nonlinear Konno-Oono system relating to electromagnetic field. *J. Opt. Quant. Elect.*, 55, 69 (2023).
22. H. Wang, Q. Zhou, A. Biswas and W. Liu. Localized waves and mixed interaction solutions with dynamical analysis to the Gross-Pitaevskii equation in the Bose-Einstein condensate. *Nonlinear Dyn.*, 106 (1), 841-854 (2021).
23. Y.Y. Yan and W.J. Liu. Soliton rectangular pulses and bound states in a dissipative system modeled by the variable-coefficients complex cubic-quintic Ginzburg-Landau equation. *Chin. Phys. Lett.*, 38 (9), 094201 (2021).

24. L.L. Wang and W.J. Liu. Stable soliton propagation in a coupled (2+1) dimensional Ginzburg-Landau system. *Chin. Phys. B*, 29 (7), 070502 (2020).
25. T.Y. Wang, Q. Zhou and W.J. Liu. Soliton fusion and fission for the high-order coupled nonlinear Schrodinger system in fiber lasers. *Chin. Phys. B*, 31 (2), 020501 (2022).
26. L. Wang, Z. Luan, Q. Zhou, A. Biswas, A.K. Alzahrani and W. Liu. Bright soliton solutions of the (2+1)-dimensional generalized coupled nonlinear Schrodinger equation with the four-wave mixing term. *Nonlinear Dyn.*, 104 (3), 2613-2620 (2021).
27. G. Ma, J. Zhao, Q. Zhou, A. Biswas and W. Liu. Soliton interaction control through dispersion and nonlinear effects for the fifth-order nonlinear Schrodinger equation. *Nonlinear Dyn.*, 106 (3), 2479-2484 (2021).
28. K. Hosseini, M. Matinfar and M. Mirzazadeh. Soliton solutions of high-order nonlinear Schrodinger equations with different laws of nonlinearities. *Regul. Chaotic Dyn.*, 26 (1), 105-112 (2021).
29. A.M. Wazwaz. Painleve analysis for new (3+1)-dimensional Boiti-Leon-Manna-Pempinelli equations with constant and time-dependant coefficients. *Int. J. Numer. Meth. Heat Fluid Flow*, 30, 4259-4266 (2020).
30. G.Q. Xu. Painleve analysis, lump-kink solutions and localized excitation solutions for the (3+1)-dimensional Boiti-Leon-Manna-Pempinelli equation. *Appl. Math. Lett.*, 97, 81-87 (2019).
31. W.Q. Peng, S.F. Tian and T.T. Zhang. Breather waves and rational solutions in the (3+1)-dimensional Boiti-Leon-Manna-Pempinelli equation. *Comput. Math. Appl.* 77 (3), 715-723 (2019).
32. M. Osman and A.M. Wazwaz. A general bilinear form to generate different wave structures of solitons for a (3+1)-dimensional Boiti-Leon-Manna-Pempinelli equation. *Math. Methods Appl. Sci.*, 42 (18), 6277-6283 (2019).

33. J.G. Liu, J.Q. Du, Z.F. Zeng and B. Nie. New three-wave solutions for the (3+1)-dimensional Boiti-Leon-Manna-Pempinelli equation. *Nonlinear Dyn.*, 88 (1), 655-661 (2017).
34. Y. Tang and W. Zai. New periodic-wave solutions for (2+1) and (3+1)-dimensional Boiti-Leon-Manna-Pempinelli equations. *Nonlinear Dyn.*, 81 (1), 249-255 (2015).
35. M. Darvishi, M. Najafi, L. Kavitha and M. Venkatesh. Stair and step soliton solutions of the integrable (2+1) and (3+1)-dimensional Boiti-Leon-Manna-Pempinelli equations. *Commun. Theor. Phys.*, 58 (6), 785 (2012).
36. I. samir, N. Badra, H.M. Ahmed and A.H. Arnous. Solitary wave solutions for generalized Boiti-Leon-Manna-Pempinelli equation by using improved simple equation method. *Int. J. Appl. Comput. Math.*, 8, 1-12 (2022).
37. M.T. Islam, M.A. Akter, J.F.G. Aguilar, M.A. Akbar and J.T. Jiménez. A novel study of the nonlinear Kadomtsev-Petviashvili-modified equal width equation describing the behavior of solitons. *J. Opt. Quant. Elect.*, 54, 725 (2022)
38. M.A. Akbar, N.H.M. Ali and T. Tanjim. Outset of multiple soliton solutions to the nonlinear Schrodinger equation and the coupled Burgers equations. *J. Phys. Commun.* 3(9), 095013 (2019).
39. M.T. Islam, F.A. Abdullah, J.F.G. Aguilar. New fascination of solitons and other wave solutions of a nonlinear model depicting ultra-short pulses in optical fibers. *J. Opt. Quant. Elect.*, 54, 805 (2022).